Appl. Phys. B 51, 222–226 (1990)

Applied Physics B Photophysics and Laser Chemistry

Investigation of Aggregation of Porphyrin Derivative Fe(TPP)Cl at Low Temperature by Time-Resolved Fluorescence Spectrum

Ju-Tao Chen and Zhen-Xin Yu

Institute for Lasers and Spectroscopy, Zhongshan University, Guangzhou 510275, People's Republic of China

Received 15 January 1990/Accepted 21 February 1990

Abstract. The time-resolved fluorescence spectrum $I(\lambda, t)$ of the porphyrin derivative Fe(TPP)Cl in solution is measured. Experiments show that when the temperature is at least 5 K above the freezing point of the solvent, the sample fluorescence does not change with temperature. But when the temperature approaches the freezing point of the solvent, the fluorescence relaxation of the high concentration sample solution is faster than that of the above normal one. Furthermore, fluorescence spectra for various times after excitation have different shapes. Analysis shows that in this case the fluorescence is composed of two components with different relaxations and spectra. The two components are attributed to monomer and aggregates respectively.

PACS: 36

Porphyrin derivatives are a large class of compounds characterized by the presence of a porphyrin ring. In many biological and medical systems, they play a very important role. For example, chlorophyll in the photosynthesis system [1], hematoporphyrin derivatives (HPD) in the photosensitive therapy of cancer [2], and so on. For decades, porphyrin derivatives have been an interesting topic of theoretical and experimental study [3].

It is noteworthy that in many cases they exist not as separate molecules, but as structures composed of interacting molecules to perform important functions [1, 2, 4]. Thus, to understand the microscopic mechanism of these important functions, it is necessary to study the structures. One of these structures is the molecular aggregate. Molecular aggregations of various porphyrin derivatives have been studied using a number of methods [5, 6]. Among them, time-resolved spectroscopy is one of the most direct and sensitive, and is thus frequently used [4, 7–11]. Molecular aggregation of chlorophyll has been extensively investigated by time-resolved spectroscopic methods [12, 13]. It is found that its fluorescence has a fast decay (relaxation time about 10 ps) owing to energy transfer and exciton migration [4, 14]. Recent time-resolved spectroscopic studies of the aggregation of hematoporphyrin derivatives have been stimulated by the photosensitive therapy of cancer. Andreoni et al. and Brookfield found that there are two decay processes in the fluorescence of some HPD, with relaxation times about 1 ns and 10 ns respectively. They suggested that this is due to HPD dimers and monomers [1, 15, 16]. Yamashita et al. found that HPD has a fast (relaxation time about 120 ps) and a slow (relaxation time about 3.6 ns) decay component, due to head-to-tail aggregates and monomers respectively. They also found evidence for Forster energy transfer from monomers to aggregates [17, 18]. Sha et al. found that there are three decay processes (lifetimes about 10 ps, 1 ns, and 10 ns respectively) corresponding to HPD monomers, dimers and aggregates [19]. In a word, fast fluorescence decay is found in various porphyrin derivatives. Generally, the fast decay is explained as the result of strong molecular interaction in aggregates.

Temperature is an important external factor in aggregate formation. Low temperature is a favorable condition for aggregation. In this paper, a time-resolved fluorescence spectrum study shows that the porphyrin derivative Fe(TPP)Cl can form aggregates at temperatures near the freezing point of the solvent, although it cannot form aggregates when the temperature is a little higher than the freezing point. An analysis and discussion of the results are also presented.

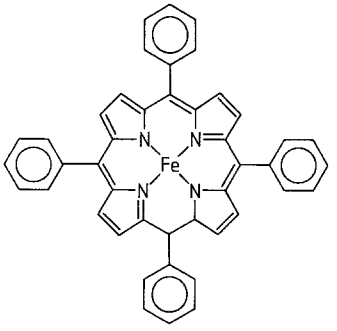

Fig. 1. Molecular structure of Fe(TPP)Cl

1. Experiment

The molecular structure of Fe(TPP)Cl is shown in Fig. 1. The sample purity is better than 99%. In the experiment, the sample is in solution, the solvent being $CHCl_3$ of AR purity.

Sample fluorescence is measured in a system with a picosecond dye laser as excitation source and a synchroscan streak camera combined with spectrograph as the measurement instrument. The laser is a Rh-6G laser with cavity dumper, synchronously pumped by second harmonic light of a cw actively mode-locked YAG laser (YAG laser pulse width about 65 ps, repetition 82 MHz, 1060 nm output at about 10 W, 530 nm output at about 1 W). The excitation pulse width is about 4 ps at a repetition rate of 800 KHz. The average power is about 10 mW at 575 nm. The scanning frequency of the synchroscan streak camera is 82 MHz and the recording range is 0.935 ns. Scanning is triggered by a PIN diode signal of the YAG laser pulse and is therefore synchronous with the dye laser output pulse. The recorded fluorescence trace is a multi-shot average (about 10^8 shots). Therefore both the signal-to-noise ratio and detection sensitivity are high. Via some alignment mirrors and a lens, the laser radiation is weakly focused on the sample cell with a beam diameter of about 0.5 mm. The average light intensity in the excitation area is about 2.5 W/cm^2, and the peak intensity is about 0.8×10^6 W/cm^2. Some measures are taken to decrease the self-absorptance effect in the high concentration solution. A lens collects sample fluorescence through a filter (>580 nm transmits) into the input slit of a spectrograph. Via the dispersion system of the spectrograph, the slit image is projected onto the input slit of the streak camera. The time-dependent fluorescence spectrum is then recorded in the streak camera. The wavelength scale of the measurement system is calibrated with a grating monochromator and the dye laser.

The time resolution of the system is determined mainly by three factors: the streak camera time resolution ΔT_s, the trigger jitter ΔT_j and the excitation width ΔT_p, which are about 2 ps, 10 ps, and 4 ps respectively. The overall time resolution $\Delta T \approx \sqrt{\Delta T_s^2 + \Delta T_j^2 + \Delta T_p^2}$ is about 11 ps. The use of the spectrograph scarcely affects the resolution; since its wavelength resolution $\Delta\nu$ is quite low, the relevant time dispersion $\Delta T_\nu \sim 1/\pi\Delta\nu$ is small in comparison with ΔT. By using a deconvolution technique, the time resolution can be increased. This technique is implemented by performing deconvolution for the recorded sample fluorescence trace with the recorded excitation laser pulse trace.

To analyze the recorded data, we take into account the effects due to the scanning mode of the streak camera. The first is the oscillating scanning effect. In the streak camera, the deflection field oscillates and is synchronized with the trigger signal. So the scanning oscillates up and down on the screen (to the right and left in the curve). If the relaxation process is longer than half of the scanning period, up and down scanning traces will overlap on the screen. However, by using this feature, we can measure long decay process (about half of the scanning period, 6.1 ns) with 0.935 ns screen range. The second effect is the multi-scanning effect. This occurs when the relaxation process is longer than the scanning period, and one decay process spans two or more sequential scans.

Low temperatures are achieved by a dewar device using liquid nitrogen as cryogen. A temperature controller combining cryogen and an electric heater is used to control the temperature. The precision of the temperature control is better than 0.5 K.

2. Results and Discussion

Firstly, the temporal behavior of the fluorescence at more than 5 K above the freezing point of the solvent is quite normal. Figure 2 (detection wavelength range is the whole fluorescence band) shows fluorescence relaxation of a low concentration sample solution at room temperature. A computer analysis shows that it is a single exponential decay with decay time

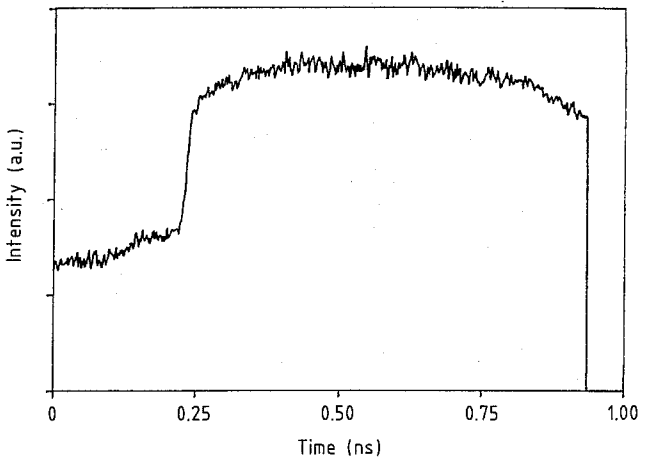

Fig. 2. Time-resolved fluorescence trace of low concentration sample solution recorded by Synchroscan streak camera. Concentration 6.5×10^{-5} mol/l. The temperature is 293 K (room temperature). Detected wavelength range is 590–800 nm

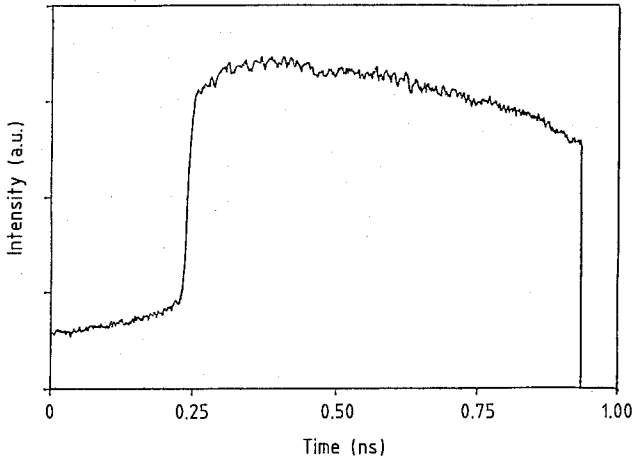

Fig. 3. Time-resolved fluorescence trace of high concentration sample solution recorded by Synchroscan streak camera. Concentration 5.2×10^{-3} mol/l. The temperature is 293 K (room temperature). Detected wavelength range is 590–800 nm

7.35 ± 0.32 ns. As the concentration increases to a relatively high value, the relaxation becomes faster and is no longer a single exponential, as shown in Fig. 3 (wavelength range is again the whole fluorescence band). In this case, the fluorescence spectrum does not change shape with time after excitation. This concentration-dependent temporal behavior is due to Forster energy transfer between excited molecules and ground state molecules, just like that occurring in high concentration chlorophyll [4].

When the temperature decreases, the temporal and spectral behavior of the fluorescence show no evident change until the temperature is near the freezing point of the solvent. When the temperature is only a little higher (about 1 K) than the freezing point of the

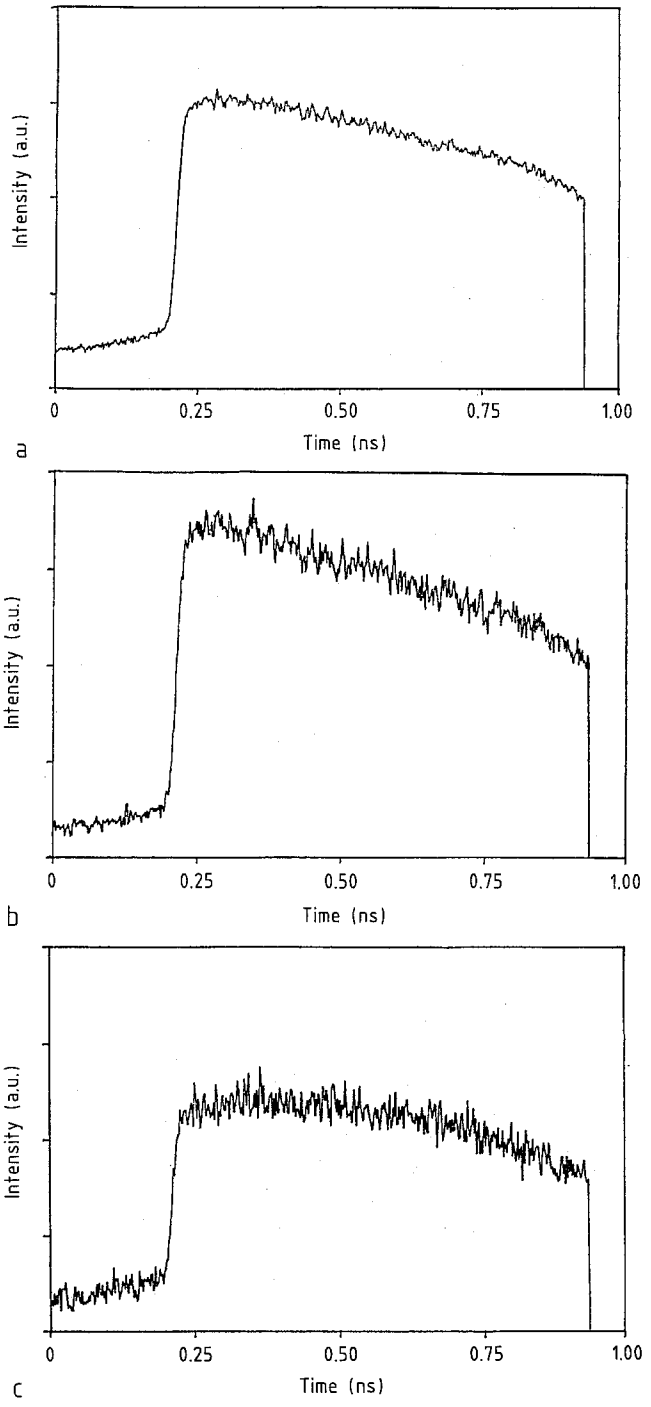

Fig. 4. Time-resolved fluorescence trace of high concentration sample solution recorded by Synchroscan streak camera. Concentration 5.2×10^{-3} mol/l. The temperature is 1 K above the solvent freezing point. Detected wavelength range is 590–800 nm for curve a, 690–710 nm for curve b, 750–800 nm for curve c

solvent, both the temporal and spectral properties are very different to the above normal case. Figure 4a (wavelength range is the whole fluorescence band) shows the relaxation curve for this case. The relaxation is faster than the normal one (Fig. 3), although the

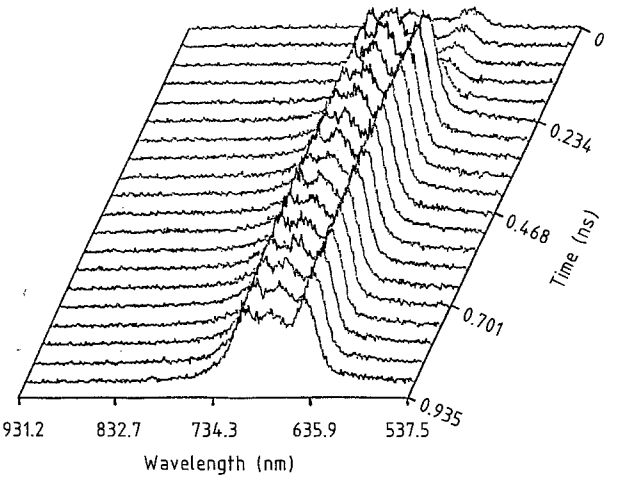

Fig. 5. Time and wavelength resolved fluorescence $I(\lambda, t)$ of sample solution. Parameters are the same as in Fig. 4a

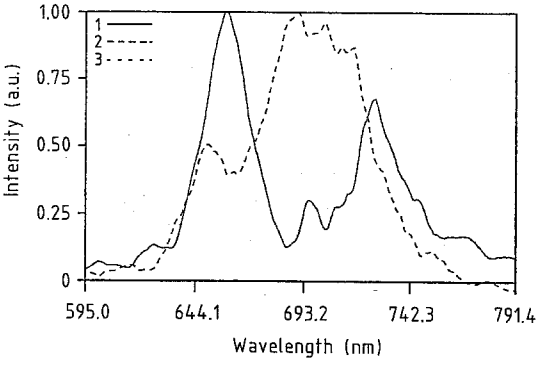

Fig. 6. Normalized fluorescence spectra of the two components fitted from $I(\lambda, t)$ of Fig. 5. Lines 1 and 2 are fluorescence spectra of the normal component and the fast relaxation component (decay time 1.49 ns) respectively

sample concentrations are the same. Figure 4b and c show the relaxation curves for detected wavelength range covering only part of the band. Figure 4b is relaxation for the center part of the band. It is obviously faster than the normal one (Fig. 3). Figure 4c shows relaxation for the red edge of the band. It is about the same as the normal one. In other words, a fast component occurs in the center part of the normal band. In the following time-resolved fluorescence spectrum results, it becomes more clear: Figure 5 shows the spectra for various times after excitation. It is obvious that a fast decay fluorescence peak appears at the center of the normal two-peak band. That is, the fluorescence is composed of two components with different spectra and relaxation times. One has a relaxation time faster than the normal one, and its spectrum is a single-peak located in the center part of the normal band. The other has a spectrum similar to the normal one. And, by noticing that Fig. 4c is very similar to Fig. 3, we see that its fluorescence relaxation is about the same as the normal one. The above results suggest that the fluorescence in this case is composed of two components with different spectra and relaxation times. Of these, the slow relaxation one is about the same as the normal one.

Experiments for lower temperature cannot be carried out, since the solvent will solidity and break the sample cell when the temperature is equal to or below its freezing point.

Of the two components, one is the normal one, which is the fluorescence of the monomer. The other is due to aggregation. The sample molecules cannot form aggregates under normal conditions. But, when the temperature is near the freezing point of the solvent, the viscosity of the solution becomes large, and some granules are formed. (In the experiment, we observed an increase in light dispersion caused by diffraction of the incident laser light by the granules.) In the following, we will analyze the occurrence of this inhomogeneity in the solvent and show that it is a favorable condition for aggregation.

To analyze the temporal characteristics, we fit the fluorescence decay curves with a function consisting of the normal decay curve (Fig. 3) and an exponential relaxation component:

$$I(t) = I_N(t) + I_g \exp\left(-\frac{t}{\tau_g}\right), \tag{1}$$

where $I_N(t)$ is the normal high concentration fluorescence relaxation (Fig. 3), τ_g is the relaxation time of the fast component, and I_g is its intensity. Fitting results show that the relaxation time of the fast component is 1.49 ns.

From the results in Fig. 5, the two components have different spectra. Here we use a fitting method to analyze the spectral characteristics of the two components. In (1), $I_N(t)$ and I_g are in practice functions of wavelength. To distinguish the wavelength structures of the two components, we fit the time-resolved fluorescence spectrum, $I(\lambda, t)$ of Fig. 5, with two sets of spectra of different relaxation processes, that is, the two relaxation processes in (1)

$$I_F(\lambda, t) = F_N(\lambda) I_N(t) + F_g(\lambda) I_g \exp\left(-\frac{t}{\tau_g}\right), \tag{2}$$

where $I_N(t)$, I_g, and τ_g are known from the previous fitting procedure. We use this expression to fit the experimental results $I(\lambda, t)$ of Fig. 5, and thus determine the spectra of the two components $F_N(\lambda)$ and $F_g(\lambda)$.

The normalized fitted results in Fig. 6 show the spectra for the two components. The fluorescence spectrum of the fast decay component is a single peak located at the center of the normal two-peaked band, whereas the slow decay component has a spectrum the

same as the normal band (i.e., the one at room temperature).

It is commonly accepted that external substituents play an important role in the aggregation of porphyrin derivatives. A suitable external substituent in a suitable position provides favorable conditions for the formation of aggregates. But Fe(TPP)Cl has no external substituent. That is, it has no intrinsic reason to form aggregates. This is why it cannot form aggregates under normal conditions. But there is a strong external reason in this case for the sample to form aggregates. When the temperature is near the freezing point of the solvent, the solvent viscosity becomes large, and some granules are formed. If there are a few sample molecules enclosed within a small granule, the distance between them will be small, so the interaction between them will become quite large. In some sense, this collection of interacting molecules within a granule is actually a type of aggregation.

Fluorescence of the sample in some commonly used inorganic solvents have also been measured. Of the many solvents, $CHCl_3$ and CH_2Cl_2 are particularly good because the sample can be dissolved in them at a concentration high enough to cause aggregation. The fluorescence of the sample in these two solvents shows no evident differences. In other solvents the sample cannot reach a concentration high enough to form aggregates.

In conclusion, the sample fluorescence at temperatures near the freezing point of the solvent is found experimentally to have two components of different relaxations and spectra. Of these, the faster relaxation component is attributed to aggregation. The other is the normal one. The formation of the aggregates is due not to intrinsic feature of the sample molecule, but to the strong external condition caused by low temperature.

Acknowledgements. We would like to thank Miss Ming Liu and Prof. Liang-Nian Ji for providing the sample, and the Computer Center of Zhongshan University for free computer use.

References

1. R.L. Brookfield: In *Primary Photoprocesses in Biology and Medicine*, ed. by R.V. Bensasson (Plenum, New York 1985) pp. 329–333
2. T.J. Dougherty, J.E. Kaufman, A. Goldfarb, K.R. Weishaupt, D.G. Boyle, M. Mittelman: Cancer Res. **38**, 2628 (1978) T.J. Dougherty, R.E. Thoma: In *Laser in Photomedicine and Photobiology*, ed. by R. Pratesi, C.A. Sacchi (Springer, Berlin, Heidelberg 1980) p. 67
3. M. Gouterman: In *The Porphyrins*, Vol. III, ed. by D. Dolphin (Academic, New York 1978) pp. 1–165
4. A.J. Campillo, S.L. Shapiro: In *Ultrafast Light Pulses* ed. by S.L. Shapiro (Springer, Berlin, Heidelberg 1977) Chap. 7
5. W.I. White: In *The Porphyrins*, Vol. V, ed. by D. Dolphin (Academic, New York 1978) pp. 303–339
6. J.C. Mialocq, C. Giannotti, P. Maillard, M. Mormenteau: Chem. Phys. Lett. **112**, 87 (1984)
7. S.R. Meech, C.D. Stubbs, D. Phillips: IEEE J. QE-**20**, 1343 (1984)
8. C.D. Tail, D. Holten, M. Gouterman: Chem. Phys. Lett. **100**, 268 (1983)
9. M. Migita, T. Okada, N. Mataga: Chem. Phys. Lett. **84**, 263 (1981)
10. M.A. Bergkamp, J. Dalton, T.L. Netzel: J. Am. Chem. Soc. **104**, 253 (1982)
11. T. Kobayashi, D. Huppert, K.D. Straub, P.M. Rentzepis: J. Chem. Phys. **70**, 1720 (1979)
12. V.H. Kollman, S.L. Shapiro, A.J. Campillo: Biochem. Biophys. Res. Commun. **63**, 917 (1975)
13. V.Z. Paschenko, S.P. Protasov, A.B. Rubin, K.N. Timofeev, L.M. Zamazova, L.B. Rubin: Biochem. Biophys. Acta **408**, 145 (1975)
14. R.S. Knox: In *Bioenergetics of Photosynthesis*, ed. by Govindjee (Academic, New York 1975) pp. 183–221
15. A. Andereoni, R. Cubeddu, S. DeSilvestri, P. Laporta, G. Jori, E. Reddi: Chem. Phys. Lett. **88**, 33 (1982)
16. A. Andereoni, R. Cubeddu, S. DeSilvestri, P. Laporta, G. Jori, E. Reddi: Chem. Phys. Lett. **108**, 141 (1984)
17. M. Yamashita, T. Honda, T. Sato, K. Aizawa: IEEE Trans. IM-**32**, 124 (1983)
18. M. Yamashita, M. Nomura, S. Kobayashi, T. Sato, K. Aizawa: IEEE J. QE-**20**, 1363 (1984)
19. W.-L. Sha, J.-T. Chen, Z.-X. Yu, S.-H. Liu: In *Laser Materials and Laser Spectroscopy*, ed. by Z.J. Wang, Z.M. Zhang (World Scientific, Singapore 1989) p. 253
20. M. Kasha: Radiation Res. **20**, 55–71 (1963)